

Production of Porous Silicon by the Method of Electrochemical Etching in Alternative Electrolytes

Zhumatova Sh.A.

*Al-Farabi Kazakh National University
Almaty, Kazakhstan*

Manakov S.M.

*Al-Farabi Kazakh National University
Almaty, Kazakhstan*

Sagidolda Ye.

*Al-Farabi Kazakh National University
Almaty, Kazakhstan*

Darmenkulova M.B.

*Al-Farabi Kazakh National University
Almaty, Kazakhstan*

Azamat R.M.

*Al-Farabi Kazakh National University
Almaty, Kazakhstan*

Alpysbayeva B.E.

*Al-Farabi Kazakh National University
Almaty, Kazakhstan*

Dikhanbayev K.K.

*Al-Farabi Kazakh National University
Almaty, Kazakhstan*

Abstract- Photoluminescent boron-doped (100)-oriented porous silicon fabricated on a p-type silicon substrate by electrochemical etching in a solution containing fluorosilicic acid and ethanol is studied. The morphological, structural, and optical properties of silicon nanostructures obtained in solutions containing $H_2(SiF_6)$ and ethanol are analyzed in comparison with the corresponding characteristics of samples formed in solutions of HF and ethanol. The morphological, structural, and optical properties were studied using scanning probe microscopy and spectrophotometry. It is shown that the porous silicon samples formed in solutions containing $H_2(SiF_6)$ and ethanol have better optical properties, in particular, they exhibit more intense photoluminescence than the samples obtained in HF-ethanol solutions.

Keywords – Porous silicon, optical properties, electrochemical etching, photoluminescence, reflection coefficient

I. INTRODUCTION

Porous silicon (PS) and, especially, nanostructured silicon are attractive materials for many practical applications, such as fabrication of electronic gas sensors [1–4], energy accumulators [5, 6], and photoelectric converters [7, 8].

The possibility of fabricating PS and nanostructured silicon using simple and inexpensive technologies with good control of the process and variability of obtained properties is the key reason for the wide practical application of these materials. Electrochemical etching of silicon is widely used for fabricating nanofilaments [9, 10] and nanoporous materials [11, 12]. A good scalability to large areas makes this method rather attractive for industrial use. There exist two main methods of electrochemical etching (both of them using solutions of fluorosilicic acid for silicon structuring), namely, chemical etching with the use of a metal catalyst and anodic etching in an electrochemical cell [13].

The first method uses metal catalysts Au, Ag, Pt for localization of silicon etching. This localization occurs due to reduction of the oxidant (usually hydrogen peroxide) via a catalytic reaction and migration of formed holes into silicon, which leads to oxidation and etching of silicon [14]. Drawbacks of this method are a high cost of noble-metal catalysts and the possibility of their incorporation into the layer during etching. Metal particles incorporated into the layer are recombination centers and may considerably deteriorate the characteristics of photoconverters with antireflecting layers of nanostructured silicon obtained by metal-induced etching. In the anodic etching method, the etching process is maintained only by external bias. Because of this, anodic etching is very attractive for formation of inexpensive porous silicon surfaces.

The porous silicon structure, properties, and morphology of the surface and pores depend on a number of factors. These factors include conduction type of single-crystalline silicon, its crystallographic orientation, specific resistivity, dopant type, illumination conditions during etching, anodizing current density, anodization duration, electrolyte composition, etc. To determine the correlation between the technological conditions of porous silicon formation and the obtained material properties, it is necessary to consider the main factors affecting the silicon structure and properties.

It is known that different etching methods and conditions affect the PS morphology and photoluminescence [15, 16]. In the present work, we fabricated for the first time PS on a p-type (100) silicon substrate by chemical etching in a solution of $H_2(SiF_6)$ and ethanol with different concentrations and studied its properties.

II. EXPERIMENTAL

Porous silicon was fabricated using single-crystalline p-type (100) silicon substrates doped with boron with a charge carrier concentration of 10^{15} cm^{-3} . Before PS fabrication, silicon substrates were degreased in hydrofluoric acid and washed with deionized water, after which they were etched for 10 min in a mixture of $H_2(SiF_6)$ and ethanol and thoroughly washed with deionized water.

We obtained three groups of PS samples at identical anodizing current densities $J = 20 \text{ mA/cm}^2$ and etching duration $t = 10 \text{ min}$. The power supply voltage was constant for all groups of samples and equal to 10 V. Etching was performed in electrolyte containing fluorosilicic acid ($H_2(SiF_6)$) and ethanol in proportions of 3 : 1, 5 : 1, and 6 : 1. The structure and properties of PS samples were measured after their storage in air for 10 days. All experiments were performed at room temperature.

The physical properties of the PS samples obtained in the new solution were compared with the properties of reference samples fabricated using solutions containing HF and ethanol in the same proportions 3 : 1, 5 : 1, 6 : 1 and at the same etching regimes.

III. EXPERIMENT AND RESULT

The surface morphology of PS films was studied using an NT-MDT NtegraTherma scanning probe microscope (SPM). The SPM images of three samples grown at 20 mA/cm^2 for 10 min are presented in Figs. 1a–1f and 2a–2f. The profiles of cross sections along the central line are shown in Figs. 1g–1i and 2g–2i. The size of crystallites and the distribution of pores on the PS layer depend on the substrate type, doping level, acid concentration, and etching time [17]. The 2D images demonstrate the presence of nanostructures surrounded by pores of irregular shape, which are randomly distributed over the entire analyzed surface. The 3D images show the roughness evolution of the same surfaces. In both cases we observe the presence of rod-like nanostructures, the number and characteristic sizes of which depend on the anodization conditions.

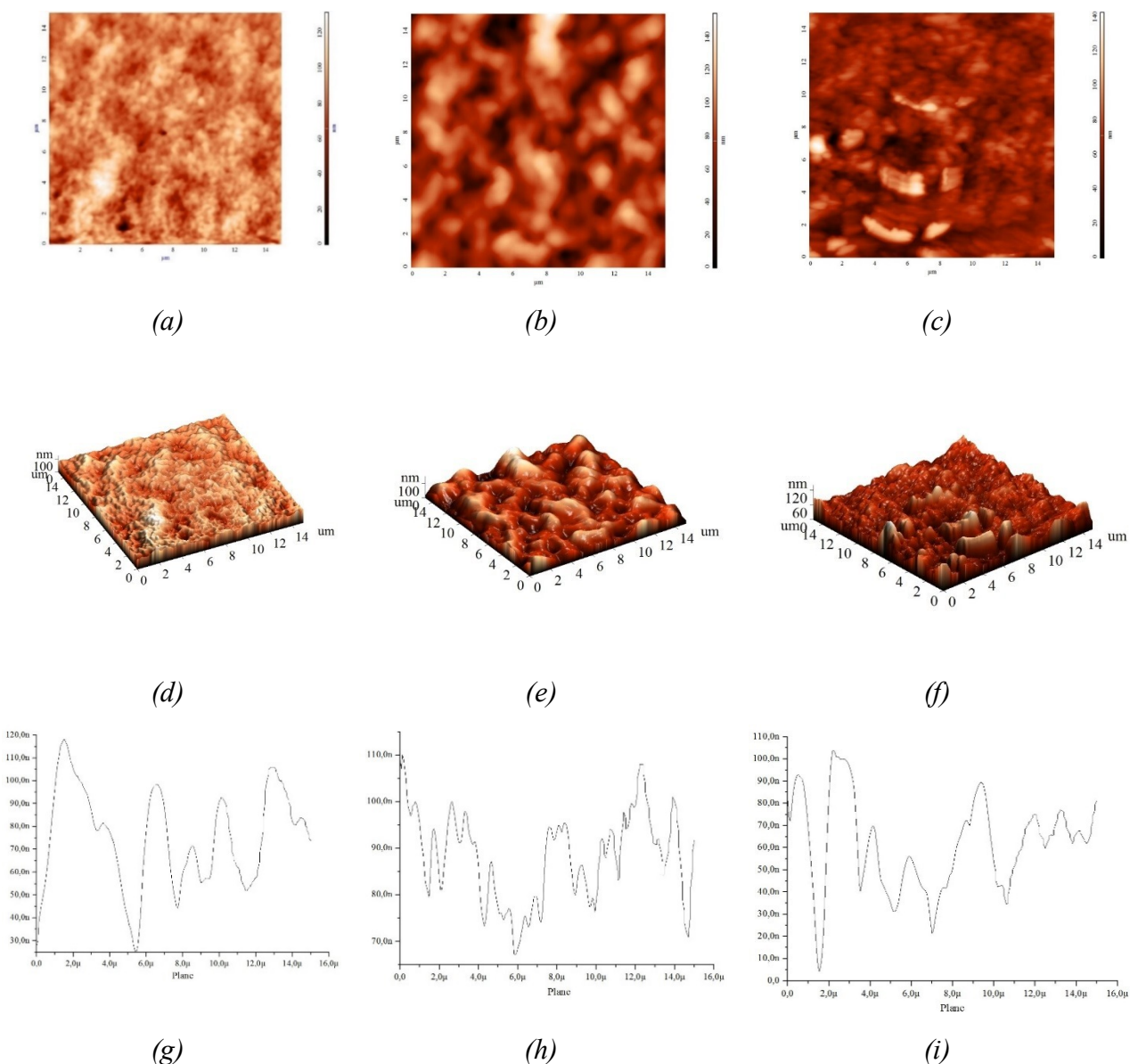


Fig. 1. SPM images of porous silicon samples obtained in $\text{H}_2(\text{SiF}_6)$ –ethanol solutions with concentration ratios of (a, d, g) 3 : 1, (b, e, h) 5 : 1, and (c, f, i) 6 : 1. (a–c) 2D images, (d–f) 3D images, (g–i) profiles of the cross sections along the central lines

The reflection spectra for all groups of samples were measured on a Shimadzu UV-3600 spectrophotometer in the range from 240 to 800 nm (Fig. 3). The character of dependences of the reflection coefficient on the active material concentration is considerably different for two electrolytes ($\text{H}_2(\text{SiF}_6)$ and HF). The reflection coefficients for the samples of the first type are 1–2% lower than for the PS samples fabricated with the use of HF. This is obviously related to a higher roughness of samples fabricated in electrolytes containing hydrofluoric acid and ethanol (Fig. 2). One can see from Fig. 3a that the reflection coefficient of the PS samples fabricated in solutions containing $\text{H}_2(\text{SiF}_6)$ and ethanol decreases with increasing concentration of $\text{H}_2(\text{SiF}_6)$. At the same time, as is seen in Fig. 3b, the samples fabricated in HF–ethanol solutions exhibit an inverse dependence, i.e., the reflection coefficient in these samples increases with increasing HF concentration. This dependence of the reflection coefficient correlates well with the

surface morphology. According to Figs. 1g–1i and 2g–2i, the average roughness calculated from the cross section profiles of samples is 9, 12, and 18 nm, respectively.

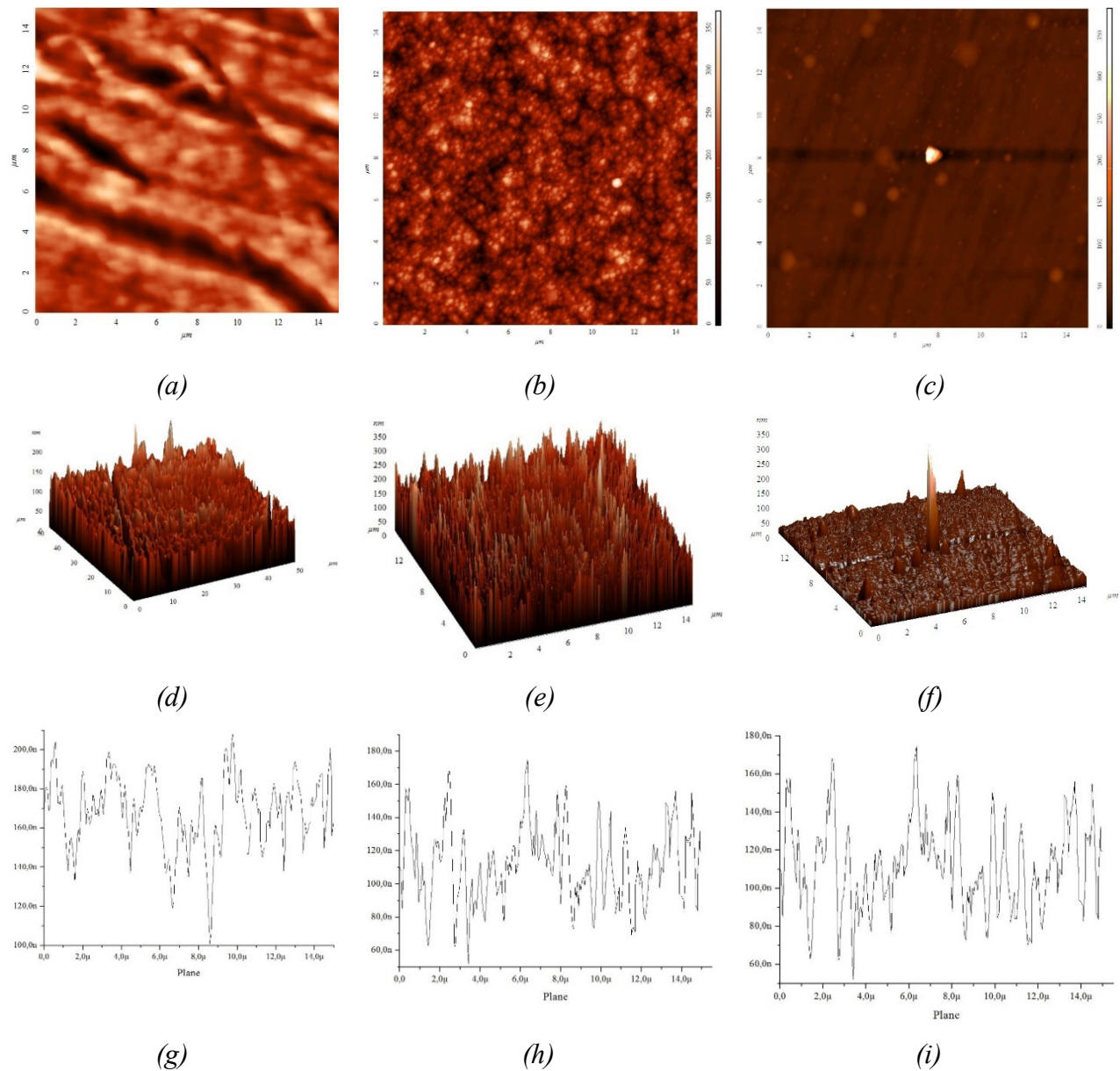
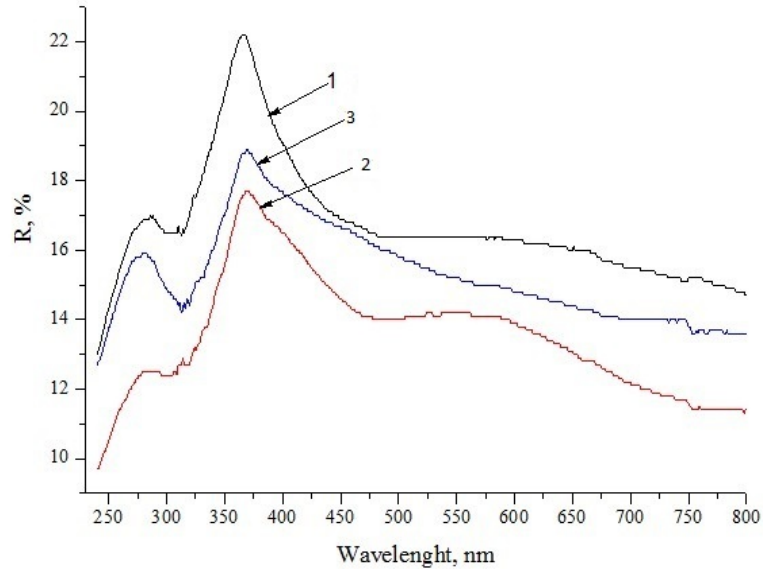


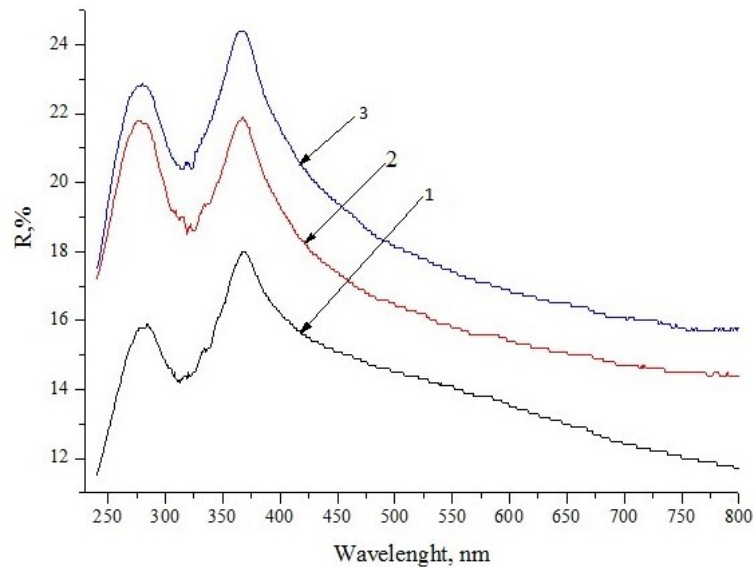
Fig. 2. SPM images of porous silicon samples obtained in HF–ethanol solutions with concentration ratios of (a, d, g) 3 : 1, (b, e, h) 5 : 1, and (c, f, i) 6 : 1. (a–c) 2D images, (d–f) 3D images, (g–i) profiles of the cross sections along the central lines

The band gap of PS increases due to the presence of nanosized silicon clusters formed near the pore walls. This is directly proved by photoluminescence (PL) in PS. The PL spectra were measured at room temperature using an NT-MDT NtegraSpectra spectrometer upon laser excitation with a power of 20 mW and a wavelength of 477 nm. The laser spot diameter on the sample was about 2 mm. Figure 4 shows the PL spectra for two types of PS samples. One can see that the PL intensity is maximum for the sample formed in the solution containing H₂(SiF₆) and ethanol in

the proportion 6 : 1 (curve 3). The PL intensity decreases for the samples obtained in the solutions with proportion 5 : 1 (curve 2) and, especially, 3 : 1 (curve 1). The PL intensity of the sample the spectrum of which is shown by curve 4 is approximately 100 times lower than the PL intensity for the sample with spectrum 3. The PL of the samples with spectra 5 and 6 has a noise-level intensity. The peaks of curve 4 lie in the range of 580–620 nm, which corresponds to a photon energy of ~ 2 eV (red spectral region) and is explained based on the quantum confinement model [9].



(a)



(b)

Fig. 3. Spectral dependence of reflection coefficients of PS samples obtained at $J = 20 \text{ mA/cm}^2$ and $t = 10 \text{ min}$ in (a) $\text{H}_2(\text{SiF}_6)$ –ethanol solutions with concentration ratios of (1) 3 : 1, (2) 5 : 1, and (3) 6 : 1, as well as in (b) HF–ethanol solutions with the same concentration ratios.

The PL spectrum of p-type porous silicon has a complex shape. This spectrum exhibits some features which may correspond both to the luminescence of nanocrystals of different sizes in the porous layer and to more complex

processes of radiative/nonradiative recombination on the surface [18]. The intensity of PL peaks depends on the concentration of $\text{H}_2(\text{SiF}_6)$ in electrolyte. The maximum intensity was observed in the sample fabricated in the solution with the concentration ratio 6 : 1 (Fig. 4, curve 3), which can be explained by a decrease in the number of nonradiative recombination centers due to a higher porosity, a more developed surface morphology, and a higher concentration of isolated nanocrystals in the silicon matrix. It should be noted that the groups of samples obtained in HF–ethanol solutions under the same anodizing conditions almost did not exhibit PL (Fig. 4, curves 4–6).

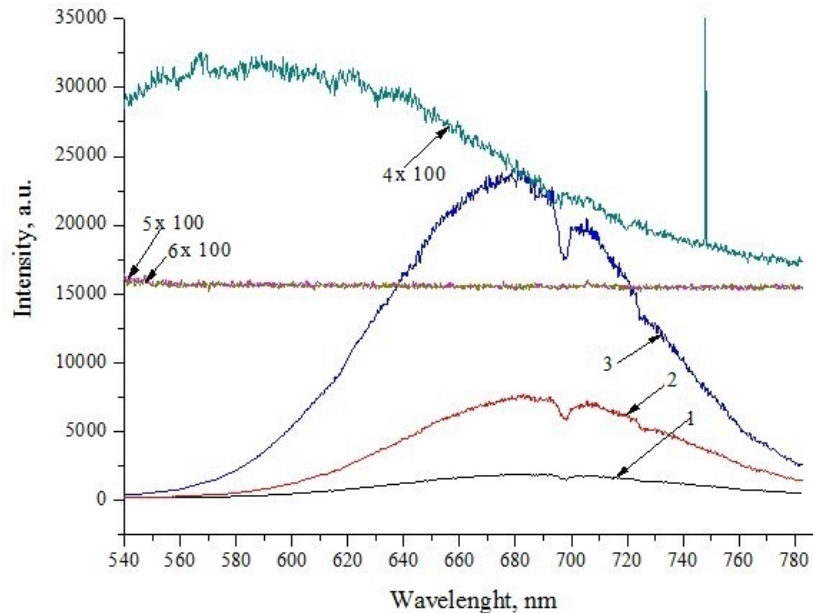


Fig. 4. PL spectra of PS samples obtained at $J = 20 \text{ mA/cm}^2$ and $t = 10 \text{ min}$ in (1–3) $\text{H}_2(\text{SiF}_6)$ –ethanol solutions with concentration ratios of 3 : 1, 5 : 1, and 6 : 1, respectively, and (4–6) HF–ethanol solutions with concentration ratios of 3 : 1, 5 : 1, and 6 : 1, respectively

IV. CONCLUSION

Porous silicon films were obtained for the first time by electrochemical etching of p-type single-crystalline silicon in electrolyte containing fluorosilicic acid and ethanol. The ratio of $\text{H}_2(\text{SiF}_6)$ and $\text{C}_2\text{H}_5\text{OH}$ components in the electrolyte for three groups of samples were 3 : 1, 5 : 1, and 6 : 1. All samples were obtained at identical anodizing current densities $J = 20 \text{ mA/cm}^2$, power supply voltage $U = 10 \text{ V}$, and etching duration $t = 10 \text{ min}$. The experimental results revealed the presence of nanostructures and pores randomly distributed over the surface. It is found that the characteristic sizes of nanostructures surrounded by nanopores depend on the anodization conditions, which makes it possible to model the reflectivity of PS layers. An increase in the average roughness of PS samples fabricated in a mixture of $\text{H}_2(\text{SiF}_6)$ and $\text{C}_2\text{H}_5\text{OH}$ from 9 to 18 nm leads to a decrease in the reflection coefficient from 16 to 14% for a wavelength of 550 nm. The maximum PL intensity is achieved at the concentration ratio between $\text{H}_2(\text{SiF}_6)$ and $\text{C}_2\text{H}_5\text{OH}$ of 6 : 1 and is two orders of magnitude higher than the maximum PL intensity in reference samples fabricated in the HF–ethanol electrolyte.

REFERENCES

- [1] Mirzaei A., Sung Yong Kang, Sun-Woo Choi, Yong Jung Kwon, Myung Sik Choi, Jae Hoon Bang, Sang Sub Kim, Hyoun Woo Kim. // *Appl. Surf. Sci. B*. 2018. V. 427. P. 215–226.
- [2] In H.J., Field C.R., Pehrsson P.E. // *Nanotechnology*. 2011. V. 22. N 35. P. 355501. doi 10.1088/0957-4484/22/35/355501
- [3] Ibraimov M.K., Sagidolda Y., Rummyantsev S.L., Zhanabaev Z.Zh., Shur M.S. // *Sensor Letters*. 2016. V.14. N 6. P. 588-591.
- [4] Manakov S.M., Ibraimov M.K., Sagidolda Y., Zhumatova S.A., Darmentkulova M.B. // *Eurasian Chemico-Technol. J*. 2019. V. 21. N 1. P. 89-93.
- [5] Peng K., Jie J., Zhang W., Lee S.T. // *Appl. Phys. Lett.* 2008. V. 93. P.033105. doi 10.1063/1.2929373
- [6] Bang B.M., Kim H., Song H.K., Cho J., Park S. // *Energy Environ. Sci.* 2011. V. 4. P. 5013–5019.
- [7] Kentaro Imamura, Takaaki Nonaka, Yuya Onitsuka, Daichi Irishika, Hikaru Kobayashi. // *Appl. Surf. Sci.* 2017. V. 395. P. 50–55.
- [8] Abdul-Hameed A.A., Mahdi M.A., Basil Ali, Selman A. M., Al-Taay H.F., Jennings P., Wen-Jen Lee. // *Superlattices and Microstruct.* 2018. V. 116. P. 27–35.
- [9] Chang S.-W., Chuang V.P., Boles S.T., Ross C.A., Thompson C.V. // *Adv. Funct. Mater.* 2009. V. 19. P. 2495–2500. doi 10.1002/adfm.200900181
- [10] Zhang M.L., Peng K.Q., Fan X., Jie J.S., Zhang R.Q., Lee S.T., Wong N.B. // *J. Phys. Chem. C*. 2008. V. 112. P. 4444 – 4450. doi 10.1021/jp077053o
- [11] Li X., Xiao Y., Yan C., Zhou K., Schweizer S.L., Sprafke A., Lee J.H., Wehrspohn R.B. // *ECS Solid State Lett.* 2013. V. 2. N2. P. 22–24.
- [12] Rajkumar K., Pandian R., Sankarakumar A., Thangavelu R., Kumar R. // *ACS Omega*. 2017. V. 2. P. 4540–4547. doi 10.1021/acsomega.7b00584
- [13] Kadlecikova M., Breza J., Vanco L., Mikolasek M., Hubenak M., Racko J., Gregus J. // *Optik*. 2018. V.174. P. 347-353.
- [14] Chang Quan Lai, Wen Zheng, Choi W.K., Thompson C.V. // *Nanoscale*. 2015. V. 7. P.11123–11134. doi 10.1039/C5NR01916H
- [15] Hu W.B., Zhao W., Fan J.L., Wu S.L., Zhang J.T. // *J. Electron. Mater.* 2016. V. 46. P. 895-902.
- [16] Mortezaali A., Ramezani Sani S., Javani Jooni F. // *J. Non-Oxide Glasses*. 2009. V. 1. N2. P. 293–299.
- [17] Hasan P.M.Z., Sajith V.K., Shah Nawaze Ansari M., Iqbal J., Alshahrie A. // *Microporous Mesoporous Mater.* 2017. V. 249. P. 176–90.
- [18] Foll H., Christophersen M., Karstensen J., Hasse G. // *Mater. Sci. Engineering Reports*. 2002. V.39. P.93-141.